The stability properties of Hill's linear periodic ODE for large parameters

Carles Simó

Departament de Matemàtica Aplicada i Anàlisi, UB, Barcelona, Catalunya

`carles@maia.ub.es`

International Conference

New Trends in Dynamical Systems (NTDS2012)

Salou, Catalunya, 201210011000

Jaume: Moltes feliçitats pels $2^2 \times 3 \times 5$

I no passa res quan hi arribes ...

The problem and the results

Consider **Hill-like** equations $\ddot{x}+(a+bp(t))x=0$, p being 1-periodic (or 2π-periodic). A very well-known example is **Mathieu** equation, where $p(t)=\cos(t)$. These equations show up in multiple applications. In particular, **to study the stability of some simple periodic orbits**.

We are interested in the study of **the stability properties** considering the parameter plane (a, b) for **large values of the parameters**:

a) We provide asymptotic estimates on the **density of the stability** in the (a, b)-plane along lines emerging from $(0, 0)$,

b) This density changes **discontinuously** at a certain direction and the **fine structure** around it is investigated asymptotically,

c) The discontinuous case of **square Hill's equation** is studied, where the density behaves differently,

d) An explanation is given of the **web-like structure** of the exponentially narrow **stability channels**, together with asymptotic estimates of the **lines forming the web**.

First we display some **motivating examples**.

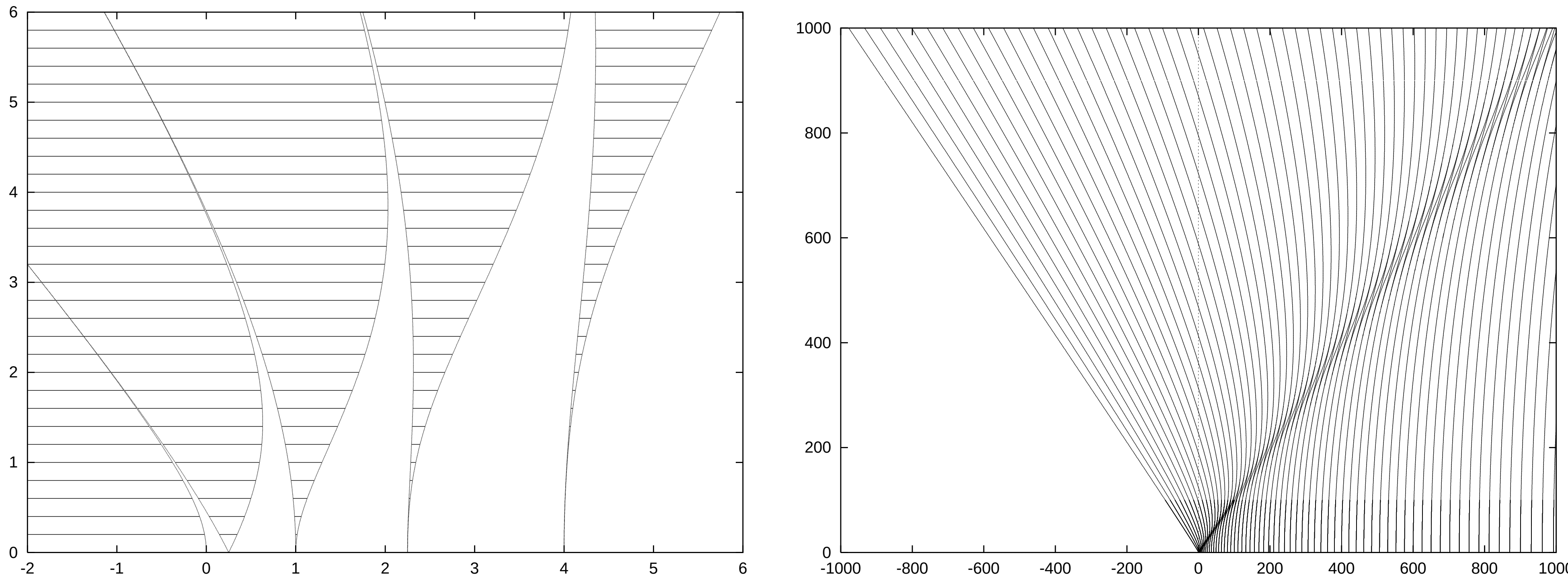

The bifurcation diagram of **Mathieu equation**. Left: some local aspects. Right: a more general plot. Parameter a (resp. b) is shown in the horizontal (resp. vertical) axis. The **shaded areas** on the left correspond to **unstable (hyperbolic) domains**. In successive plots we do not shadow domains.

Note that beyond being **reversible**, $p(t) = p(-t)$, function p is **antisymmetric** with a suitable shift: $p(t - \pi/2) = -p(-(t - \pi/2))$. Hence the **diagram is symmetric** with respect $(a, b) \leftrightarrow (a, -b)$.

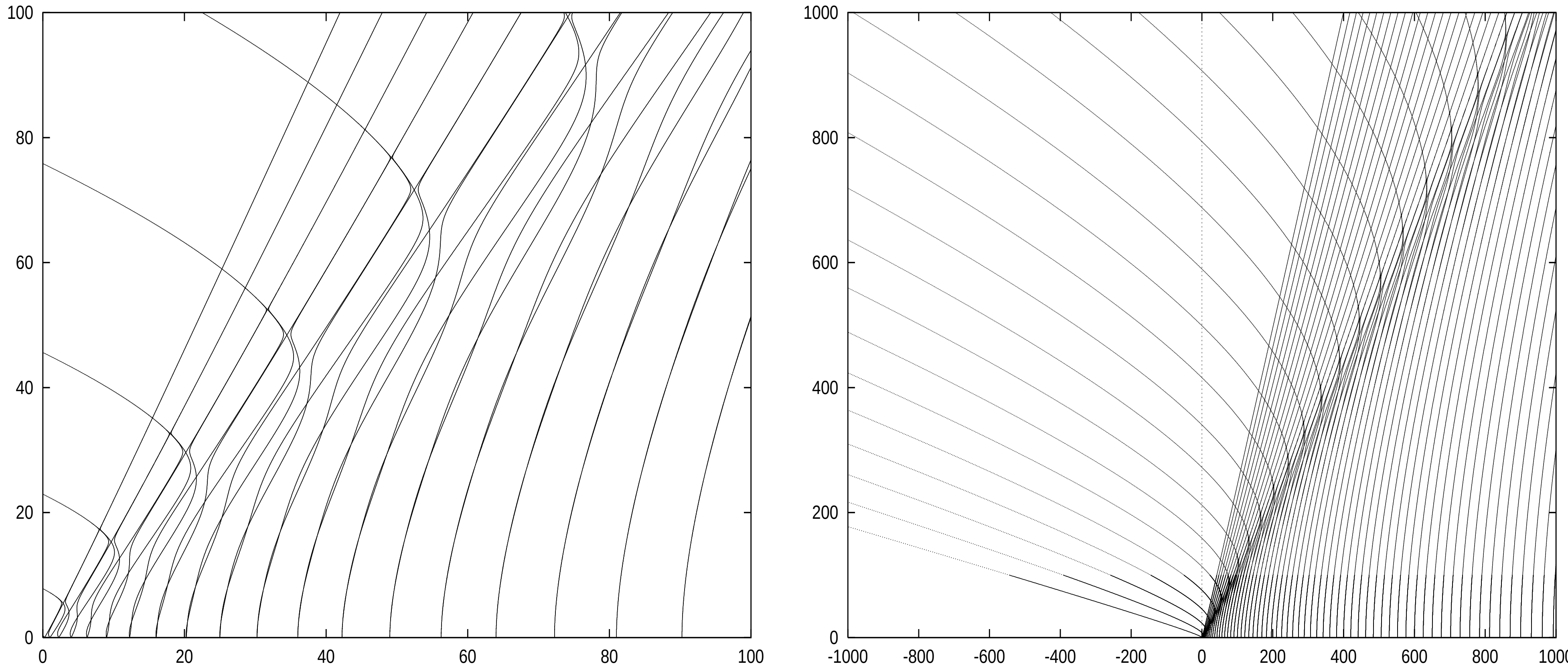

Some bifurcation diagrams of Hill's equations: **Ince equation**

$$p(t) = \frac{1}{1+\mu^2}\frac{\cos(t)-\nu}{(1-\nu\cos(t))^2}, \qquad \nu = \frac{2\mu}{1+\mu^2},$$

where the value $\mu = 0.6$ has been used.

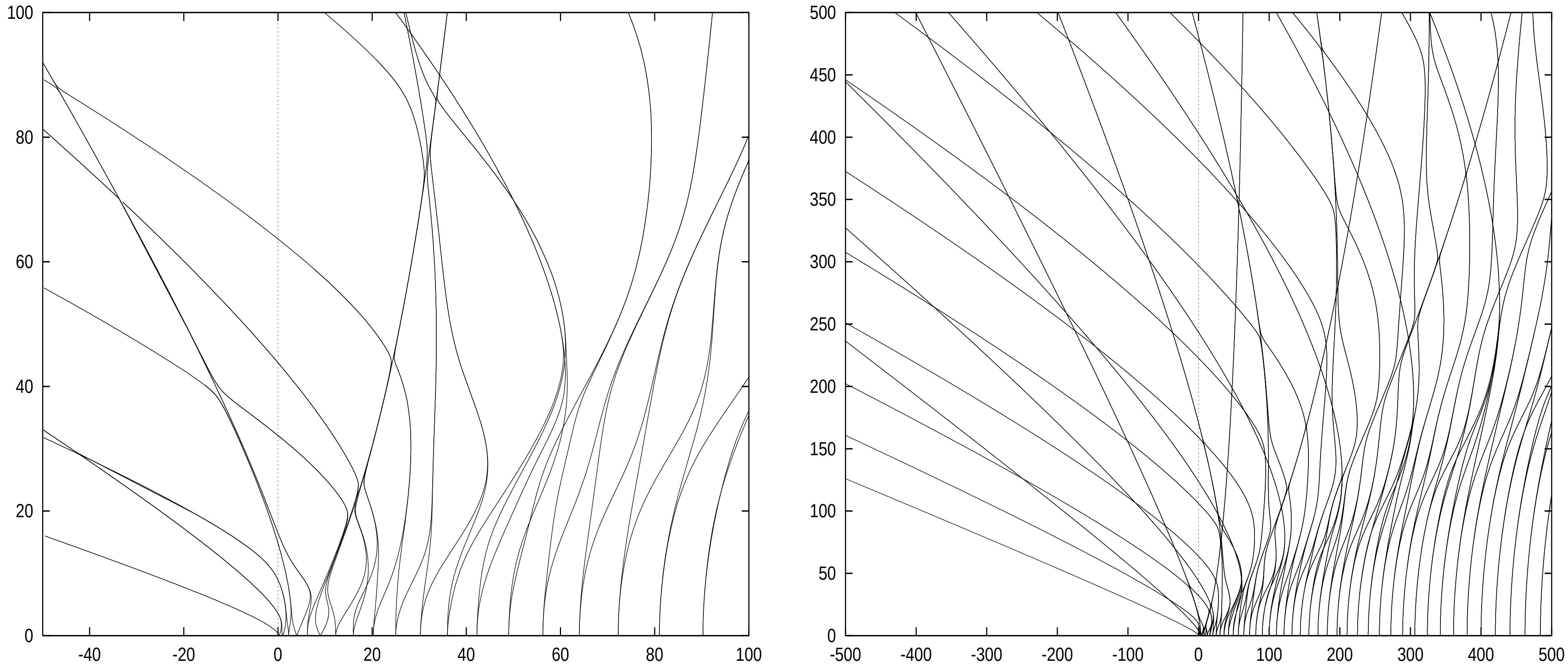

Some bifurcation diagrams of Hill's equations: Function

$$p(t) = \cos(t) + \cos(2t) + \cos(4t) + 1.5\cos(6t).$$

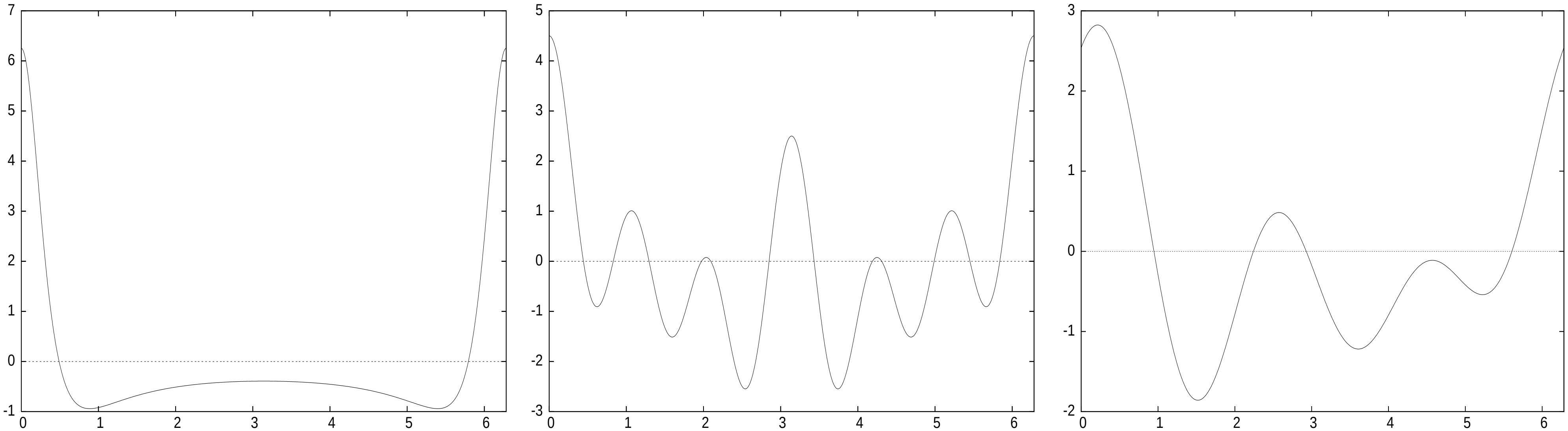

Plots of the **functions** p used in the two previous examples (left: Ince; middle: function containing up to the sixth harmonic) and the next one (**non-reversible, non-antisymmetric**) with

$$p(t) = \cos(t) + \cos(2t) + \cos(3t - 1).$$

By changing the ratio b/a we can have $a + bp$ **all above or below the axis, tangent minima and tangent maxima**. All these cases play a relevant role.

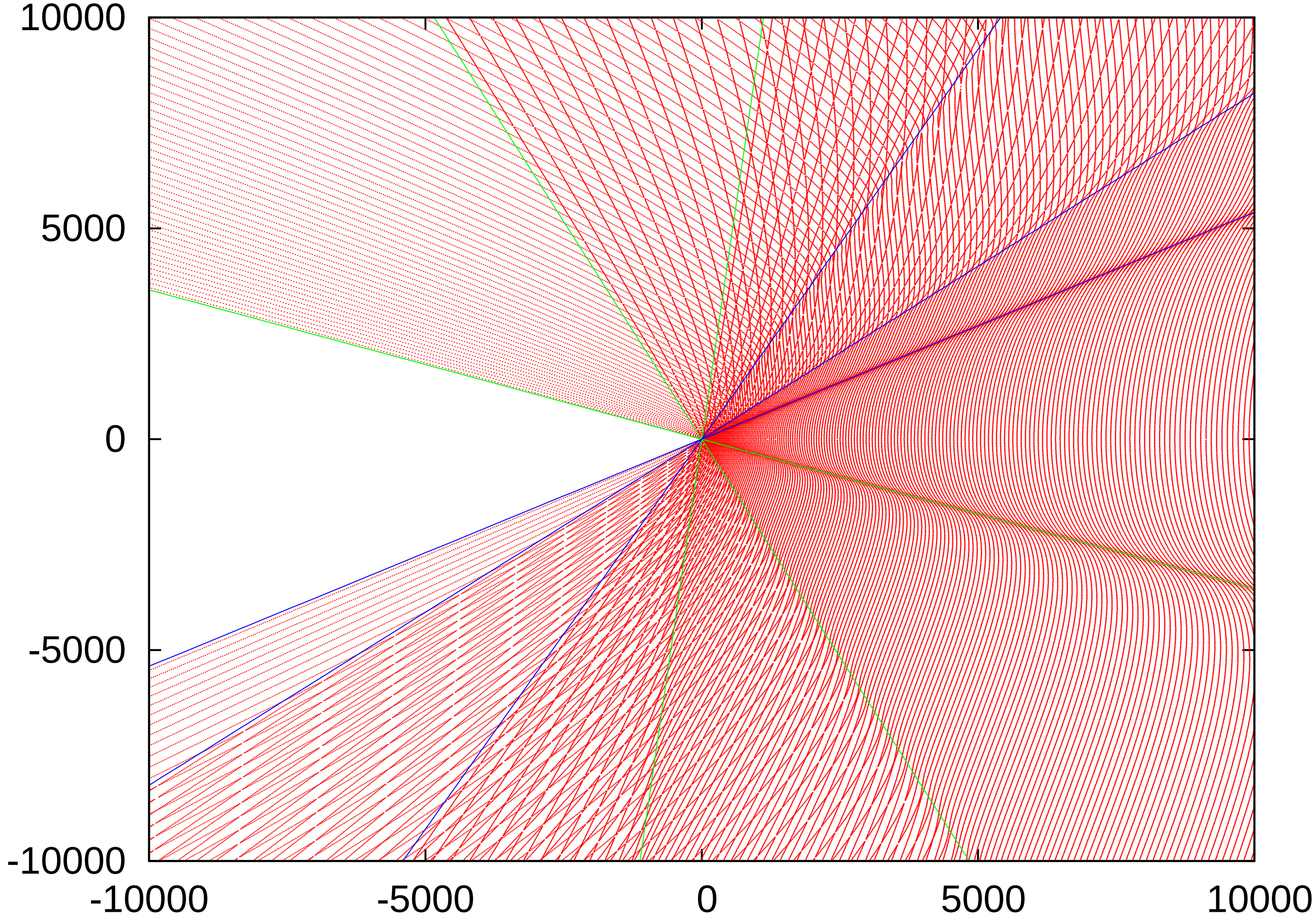

A part of the bifurcation diagram for a **non-reversible, non-antisymmetric** function p. The plot of the function is used as example of several regions of positivity. The number of regions with a different pattern is 12. **Blue and green lines** refer to **tangent to minima and maxima**.

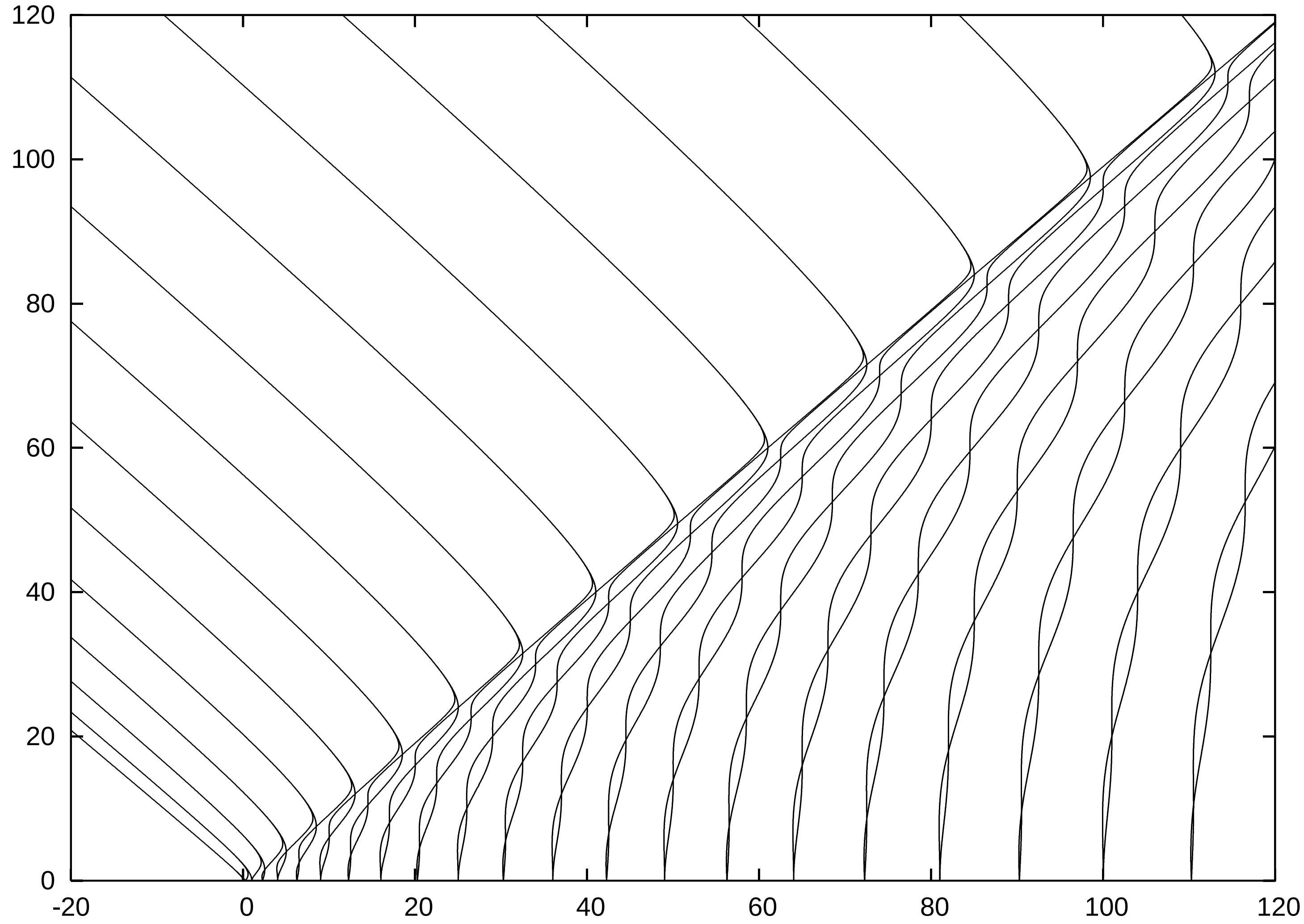

A part of the bifurcation diagram for the **square wave**:

$$\ddot{x} + (a + b\,\mathrm{sign}(\sin(2\pi t)))x = 0.$$

Compare with the previous plots.

We introduce ω and χ:

$$a = \omega^2 \cos(\chi), b = \omega^2 \sin(\chi).$$

We shall also use in the future the small parameter $\varepsilon = 1/\omega$.
Let $L(\chi; k)$ be the segment of length k from $(0, 0)$ and argument χ.

Density of a set S: limit (if it exists)

$$\rho(\chi) = \lim_{k \to \infty} \frac{|S \cap L(\chi; k)|}{k}.$$

Theorem 1 *Assume p of class C^2, with zero average. Also assume that p only has non-degenerate extrema. Denote $p_m = \min p(t)$ and $p_M = \max p(t)$. Let S_p be the set of (a, b) for which there is stability. Then*

$$\rho(\chi) = \begin{cases} 1 & \textit{if} \quad \tan(\chi) \quad \textit{is inside the interval} \quad I := (-p_M^{-1}, -p_m^{-1}); \\ \frac{1}{2} & \textit{if} \quad \tan(\chi) \quad \textit{is one of the endpoints of } I \\ 0 & \textit{if} \quad \tan(\chi) \quad \textit{is outside } I. \end{cases}$$

Theorem 1 follows from next one.

Introduce $q(t) = \cos(\chi) + p(t)\sin(\chi)$ and consider

$$\ddot{x} + \omega^2 q(t) x = 0, \quad q(t+1) = q(t).$$

For a **given function q define**

$$r = r(q) = \lim_{\Omega\to\infty} \frac{1}{\Omega} |\{\omega : \text{Hill's equation is stable}, \ 0 < \omega < \Omega\}|$$

Theorem 2 *Assuming that the function q is of class $\mathcal{C}^2$ with only one absolute minimum, non-degenerate, then r satisfies the following:*

$$r(q) = \begin{cases} 1 & \textit{if for all } t \textit{ one has } q(t) > 0 \ ; \\ \frac{1}{2} & \textit{if } \ q \geq 0 \ \textit{ and there exist isolated zeros with } \ddot{q} > 0; \\ 0 & \textit{if } q \textit{ is negative in some interval.} \end{cases}$$

The first case follows from **averaging/adiabatic invariance** and control of the width of the unstable domains. The third needs to split the full interval in **different pieces with emphasis on hyperbolic domains**. The middle case is **much more delicate** and requires the use of some **special functions**. The case $q < 0$ everywhere is an easy undergraduate exercise.

The previous theorems lead to some **natural questions**.

a) Looking at q as depending on χ the function $\rho(\chi)$ has a **discontinuity** at the endpoints of I or **critical lines**. We like to know what is **fine structure of** ρ near these lines. This requires **appropriate scalings**.

b) **How fast** do we tend to the limits given by the theorem? And **how this depends on the regularity of** q?

c) Which kinds of modifications have to be introduced to discuss the case of **several absolute minima** with either the same or different **order**?

Beyond possible discussions on results on these items, it is worth to say that the answers mainly rely on a careful use of **the tools introduced to prove the main theorems**.

d) A special problem appears when there is complete **lack of regularity**, as it happens for the **square wave Hill's equation**. We shall present results. Both **results and methods** largely differ from the ones in the smooth case.

Below a critical line: no change of sign

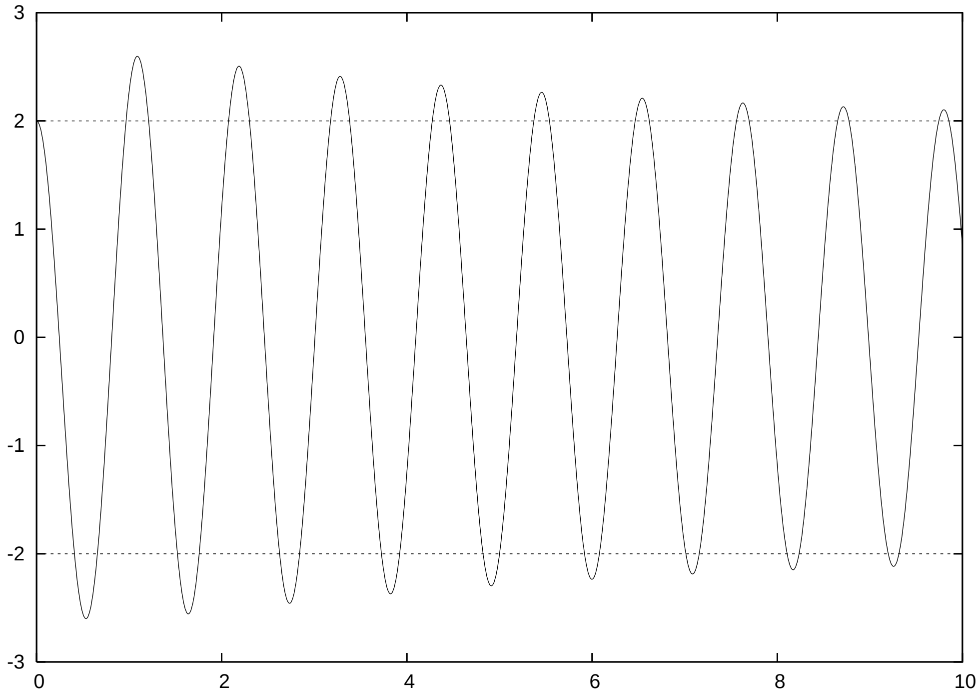

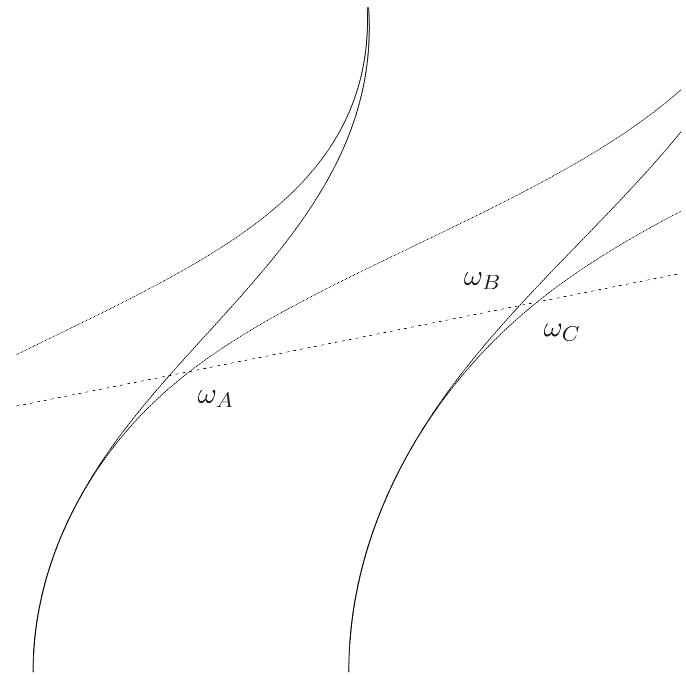

For a line **below but close** to the critical line the trace $\mathrm{Tr}\, F_\omega$ tends to **oscillate periodically** in ω, with an amplitude **tending to 2**. On the right plot we indicate ω_A on the right hand side of an instability gap and the next gap $[\omega_B, \omega_C]$.

Hint: Change from $\dot{x} = -\omega y, \quad \dot{y} = \omega q(t) x$ by $q^{1/4} x = \sqrt{I} \cos\theta$, $q^{-1/4} y = \sqrt{I} \sin\theta$ and use the fact that θ is a fast variable.

Turning to the case of **change of sign** we prove, in fact the equivalent statement:

Theorem 3 *Consider Hill's equation*

$$\ddot{x} + \omega^2 q(t) x = 0, \qquad q(t+1) = q(t)$$

with q of class $\mathcal{C}^2$. Assume that q **changes sign twice, in a transversal way**. *That is, it has only one negative minimum. Then $r(q) = 0$, i.e., the set of stable ω is sparse.*

The general case, with several changes of sign, runs completely similar.

Hence we **split the monodromy matrix** as

$$F_\omega = C_u \circ M_- \circ C_d \circ M_+.$$

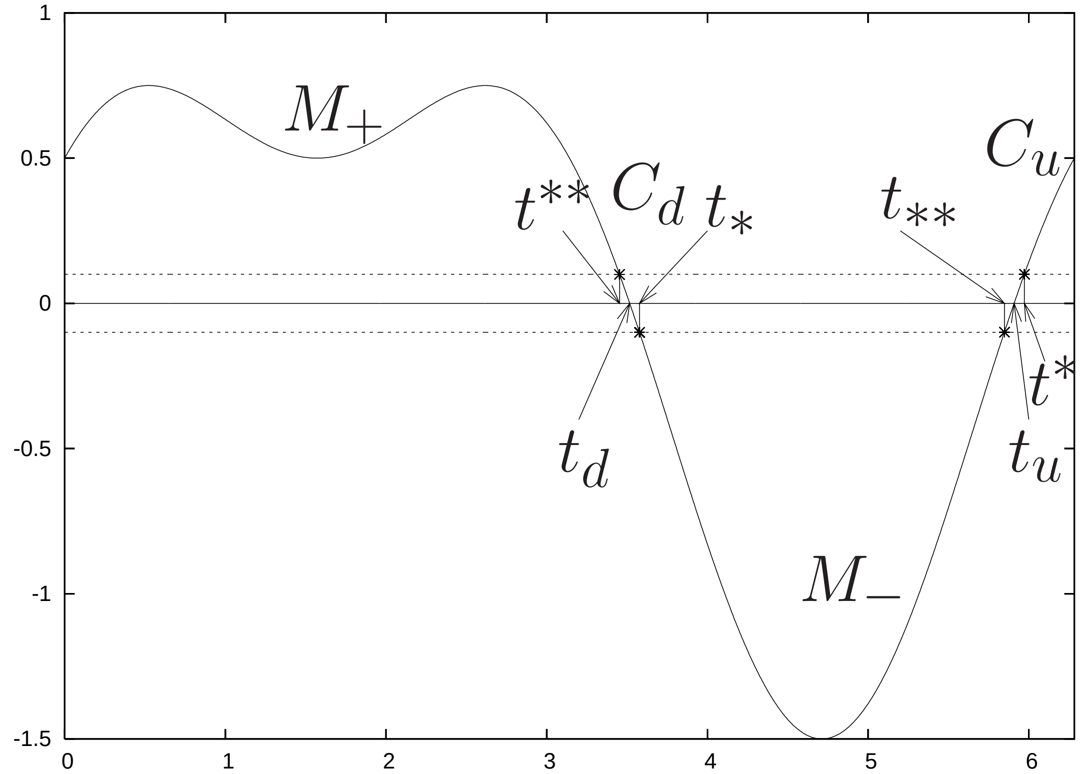

Graph of q in the case of **transversal (one down, one up) sign changes**. The Poincaré map F_ω is decomposed as $F_\omega = C_u \circ M_- \circ C_d \circ M_+$. Here M_+, M_- are the **strongly elliptic** resp. **hyperbolic** parts and C_u, C_d are the **transitions through the sign-change** of q in 'upward' resp. 'downward' direction.

For the case of change of sign, the **Poincaré matrices in the domains** $q(t) > 0, q(t) < 0$ are of the form

$$M_+ = \begin{pmatrix} \cos(\omega J) + O(\varepsilon) & -\hat{q}^{-1/2}\sin(\omega J) + O(\varepsilon) \\ \hat{q}^{1/2}\sin(\omega J) + O(\varepsilon) & \cos(\omega J) + O(\varepsilon) \end{pmatrix}, \quad J = \int_{t^*}^{t^{**}} \sqrt{q(t)}\, dt.$$

$$M_- = \begin{pmatrix} C & -\hat{q}^{-1/2} S \\ -\hat{q}^{1/2} S & C \end{pmatrix}, \quad C = \cosh(c_*\omega), \quad S = \sinh(c_*\omega),$$

being c_* a constant independent of ω and we have **skipped the error terms** in M_-. The value of $\hat{q}$ is $\hat{K}\varepsilon^{2/3}$ for some large, fixed, $\hat{K}$.

It is essential to select the **transition intervals** of length $O(K\varepsilon^{2/3})$, in generic cases, where K is large but fixed (independent of ε). In them we relate the C_u, C_d matrices to **Airy's equation**

$$\frac{d^2 w}{dz^2} + zw = 0.$$

To analyse C_u, C_d and also **near tangency**, it is useful to introduce **generalised and shifted Airy–like equations**

$$d^2w/dz^2 = -(D + |z|^\gamma)w$$

with D finite, $\gamma > 0$ and **fundamental solutions** $f_{\gamma,D}(z), g_{\gamma,D}(z)$ such that $f_{\gamma,D}(0) = 1,\ df_{\gamma,D}/dz(0) = 0,\ g_{\gamma,D}(0) = 0,\ dg_{\gamma,D}/dz(0) = 1.$

We analyse the **local behaviour near a minimum** of the form

$$p(t) = d + c|t|^\gamma(1 + o(1)), \qquad \dot{p}(t) = \gamma c\,\mathrm{sign}\,(t)|t|^{\gamma-1}(1 + o(1)).$$

(**locally near reversible**). In particular using **suitable scalings** we obtain.

Lemma *In Hill's equation assume p has an absolute minimum located at $t = 0$ and that $p(t) = m+n|t|^\gamma(1+o(1))$ locally, with $m < 0$, $n > 0$, $\gamma > 0$. For a fixed large value of a let $b_{\mathrm{crit}} = -a/m$ the critical value such that q is tangent to 0 at 0. Then the transition from mostly stable systems to mostly unstable is done for a range of b around b_{crit} with size $O(a^{2/(2+\gamma)})$.*

What happens at exact tangency?

Theorem 4 *If p behaves like $m+n|t|^{\gamma}(1+o(1))$ at an absolute minimum, assumed to be unique, and $\dot{q}$ like $\gamma n\,\mathrm{sign}(t)|t|^{\gamma-1}(1+o(1))$, where $\gamma > 0$, then the density at the critical line is $\frac{2}{\gamma+2}$.*

This amounts to a study of the generalised Airy equation with $D = 0$, i.e. $d^2x/ds^2 + |s|^{\gamma}x = 0$.

Sketch of the proof:

1) After some expansions one has a **fundamental solution** given by

$$x_1(s) = \Gamma\left(\frac{\gamma+1}{\gamma+2}\right)\left(\frac{z}{2}\right)^{-\nu_1} J_{\nu_1}(z), \qquad x_2(s) = \Gamma\left(\frac{\gamma+3}{\gamma+2}\right)\left(\frac{z}{2}\right)^{-\nu_2} J_{\nu_2}(z),$$

where J_ν denote **Bessel functions of the first kind**, $\nu_1 = -1/(\gamma+2)$, $\nu_2 = 1/(\gamma+2)$ and $z = 2s^{(\gamma+2)/2}/(\gamma+2)$.

2) Use **Hankel's asymptotic expansions** for fixed ν and large z and recall $\Gamma\left(1 - \frac{1}{\gamma+2}\right)\Gamma\left(\frac{1}{\gamma+2}\right) = \frac{\pi}{\sin(\pi/(\gamma+2))}$, to obtain an expression for the N giving the **passage near the tangency**, whose elements are

$$n_{1,1} = n_{2,2} \;=\; -\frac{\cos(2z)}{\sin(\frac{\pi}{\gamma+2})},$$
$$n_{2,1} \;=\; \alpha\Gamma\left(1-\frac{1}{\gamma+2}\right)^2 \hat{\gamma}^2\frac{1}{\pi}\sin(2(z-\delta)),$$
$$n_{1,2} \;=\; \alpha^{-1}\Gamma\left(\frac{1}{\gamma+2}\right)^2 \hat{\gamma}^{-2}\frac{1}{\pi}\sin(2(z+\delta)),$$

where $\hat{\gamma} = (\gamma+2)^{\frac{1}{2}-\frac{1}{\gamma+2}}$ and $\delta = \frac{\pi}{4} - \frac{\pi}{2(\gamma+2)}$.

3) Multiply N by the M_+ part **coming from the domain** $q > 0$ to obtain F_ω, whose **trace** can be written as

$$\sin\left(\frac{\pi}{\gamma+2}\right)\mathrm{Tr}\, F_\omega =$$

$$\left[-2\cos(\omega J)\cos(2z) + \sin(\omega J)\{\hat{P}\sin(2(z+\delta)) - \hat{Q}\sin(2(z-\delta))\}\right],$$

where $\hat{P}\hat{Q} = 1$ and the dominant term in $\hat{P}$ is equal to 1.

4) Shift slightly z to z^* such that

$$\hat{P}\sin(2(z^*+\delta)) - \hat{Q}\sin(2(z^*-\delta)) = 2\sin(2z^*).$$

Then the **trace becomes**

$$\mathrm{Tr}\, F_\omega = -2\cos(\omega J + 2z^*)/\sin(\pi/(\gamma+2))$$

and the **result follows** easily.

What happens at the transition?

We confine our study to the **generic case** $\gamma = 2$ with varying D. In that case the main role is played by the **parabolic cylinder equation**

$$\frac{d^2w}{dz^2} + \left(\frac{1}{4}z^2 - a\right) w = 0.$$

We apply techniques similar to the ones used for the tangency to obtain

Theorem 5 *Near the critical line Hill's equation, for* $\mathcal{C}^2$ *functions* q *with generic minima, can be written in the form* $\ddot{x}+\omega^2\left(ct^2-\frac{\hat{d}}{\omega}+\mathcal{O}(t^3)\right)x=0.$ *Increasing* $\hat{d}$ *we cross the line from top to bottom. Then the density of stability as a function of* $c, \hat{d}$ *tends to*

$$\rho(c,\hat{d}) = \frac{1}{\pi}\arccos\left(\tanh\left(\frac{\pi\hat{d}}{2\sqrt{c}}\right)\right)$$

when $\omega \to \infty$.

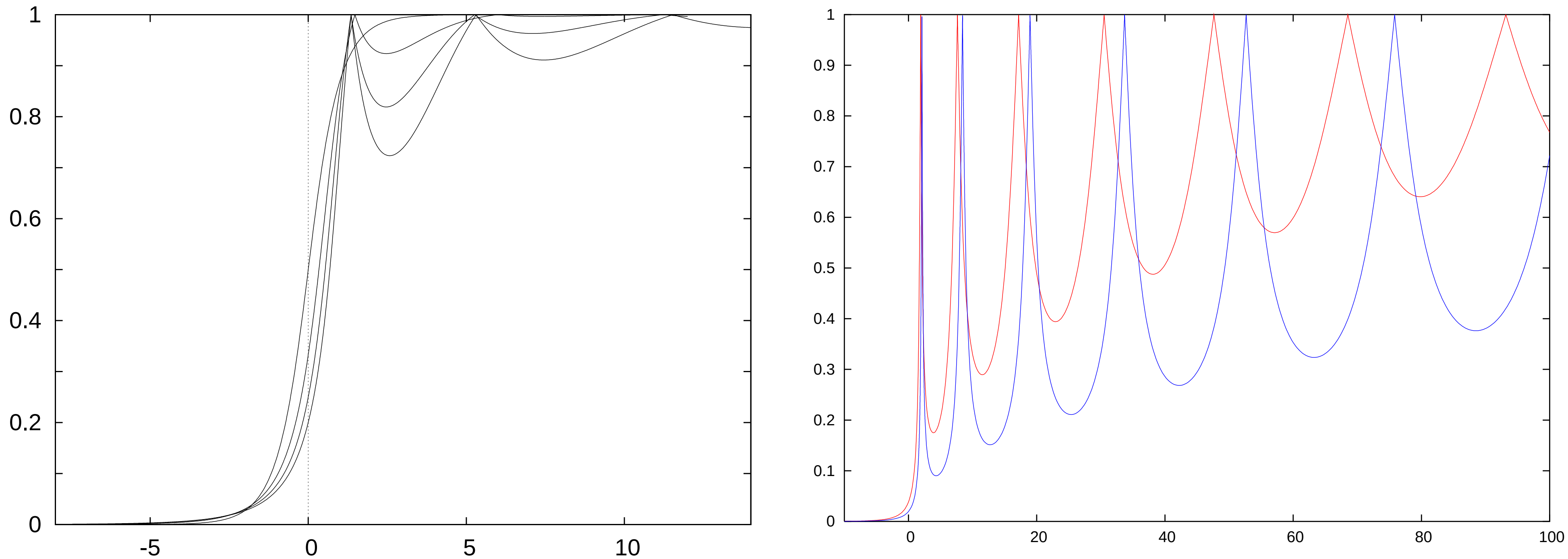

Left: The **transition functions**, showing the variation of ρ corresponding to different γ for the **generalised and shifted Airy equation** as a function of D. The values of γ when crossing $D = 0$ are 2,4,6,8, from top to bottom. The value 2 corresponds to theorem 5. Right: Similar plots for **large order of tangency**: $\gamma = 50, 100$.

We can illustrate the behaviour for some 2π periodic functions of **Mathieu-like** type, like $d^2x/dt^2+(\omega^2(2\sin(t/2))^k+D\omega^{4/(2+k)})x=0$, $\gamma=k=2,4,6,8$.

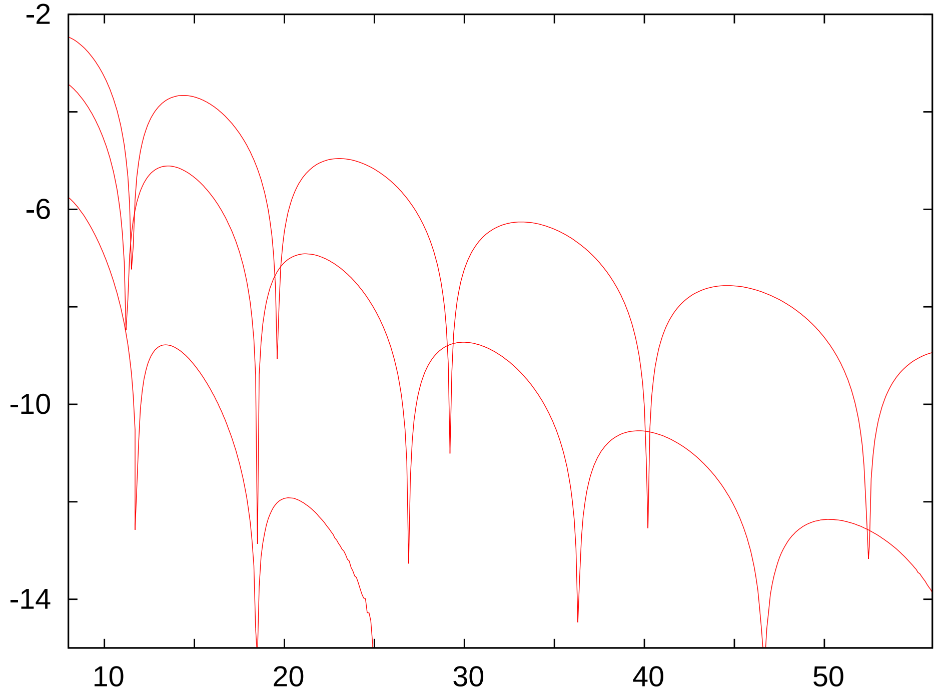

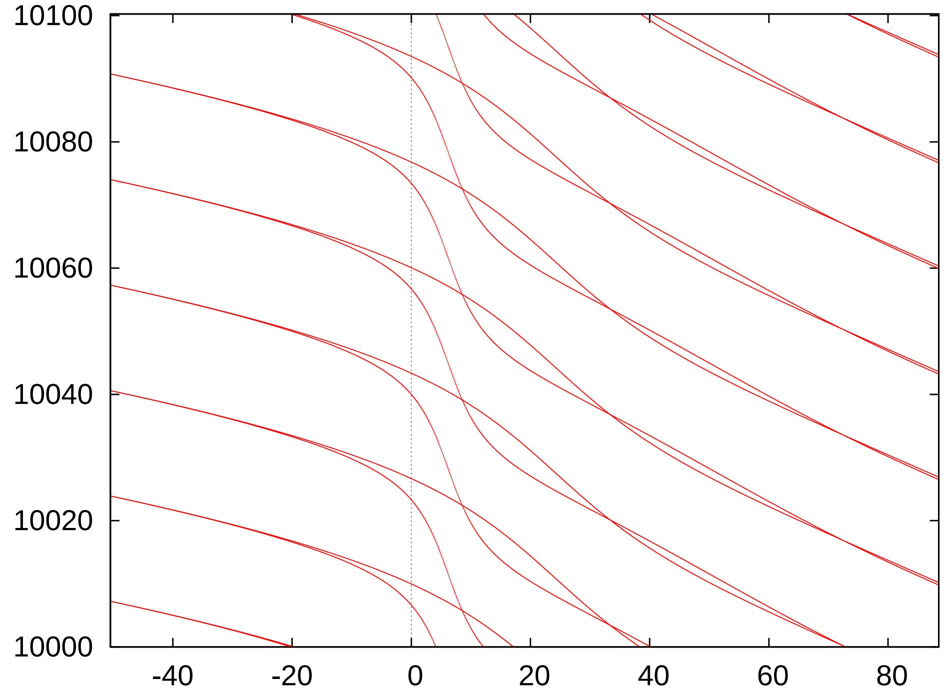

As given by Theorem 5 and seen in the previous figure for $\gamma = 2$ the function $\rho(D)$ is **monotonically increasing**, while for $\gamma > 2$ seems to be not true. It reaches the **value 1** for intermediate D. The left plot shows $\log(1-\rho(D))$ **as a function of** D for values of D on a grid.

The values $\rho(D) = 1$ are associated to **end points of instability pockets**, a known fact well studied in the **perturbative regime**. The right plot **displays the pockets** for the last example in previous page and $k = 8$ in the **variables** $(a - b, b)$ for some large values of the parameters.

The square wave Hill's equation

As a simple case with **discontinuous** p we consider the **square wave**. Putting $b = a(1-\delta)$ we analyse the **transition** when δ goes from 1 to 0. Let $\omega_1^2 = a(2-\delta)$ and $\omega_2^2 = a\delta$. An undergraduate computation gives the **trace of the monodromy matrix** as

$$\mathrm{Tr}\ P_\delta = 2\cos\omega_1\cos\omega_2 - (\omega_1/\omega_2 + \omega_2/\omega_1)\sin\omega_1\sin\omega_2.$$

If $\omega_2/\omega_1 \notin \mathbb{Q}$ we can use **Birkhoff ergodic theorem** to obtain

$$\rho(\delta) = \frac{1}{4\pi^2}\lambda\left(\{(\theta_1,\theta_2)\in\mathbb{T}^2 \mid |\cos\theta_1\cos\theta_2 - B(\delta)\sin\theta_1\sin\theta_2| < 1\}\right).$$

Here λ is the **Lebesgue measure on** $\mathbb{T}^2$ and $B(\delta) = 1/\sqrt{\delta(2-\delta)}$.

Lemma *The function ρ is monotonically increasing in δ. The limit values are*

$$\rho(\delta) = 1 - 4(1-\delta)/\pi^2 + O((1-\delta)^3), \quad \text{for} \quad \delta\to 1,$$

$$\rho(\delta) = \frac{2}{\pi^2}\sqrt{2\delta}\left(-\log(\delta) + O(1)\right), \quad \text{for} \quad \delta\to 0.$$

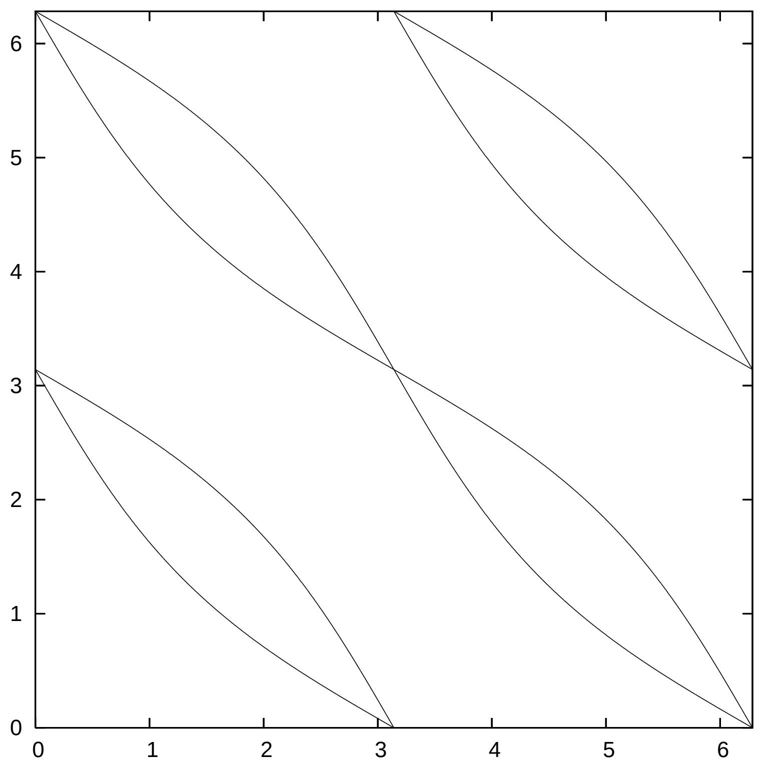

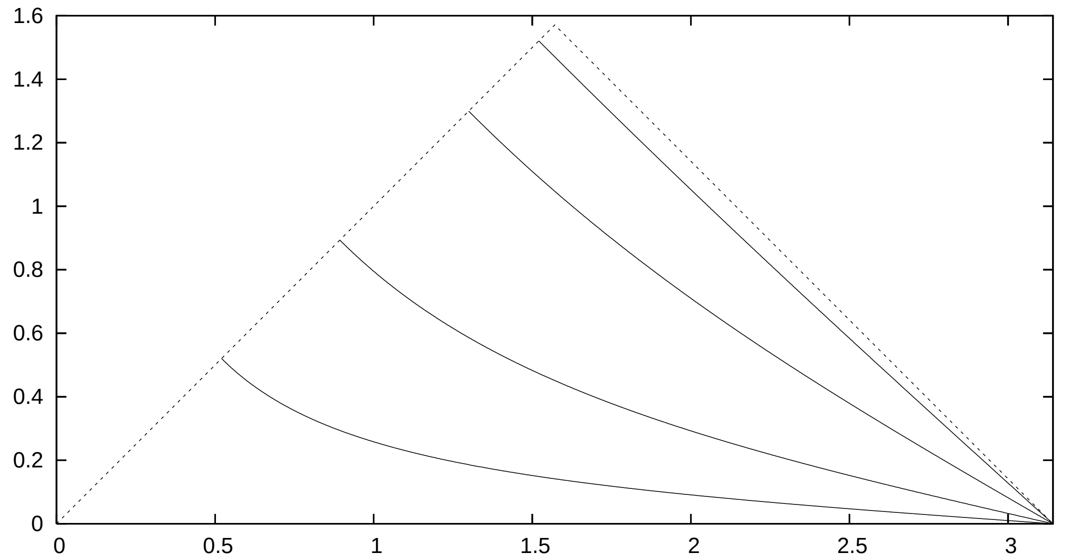

Left: Typical shape of the curves Tr $P_\delta(\theta_1, \theta_2) = \pm 2$. The area inside the **lenses** corresponds to instability, i.e., where $|\mathrm{Tr}| > 2$. Right: the $\mathcal{B}$ curves, **boundaries of the lenses** are displayed in 1/16 of $\mathbb{T}^2$ for $\delta = 0.9,\ 0.5,\ 0.1,\ 0.01$ from top to bottom.

The point in $\theta_1 = \theta_2$ is given by $\arccos(\sqrt{(B(\delta)-1)/(B(\delta)+1)})$.

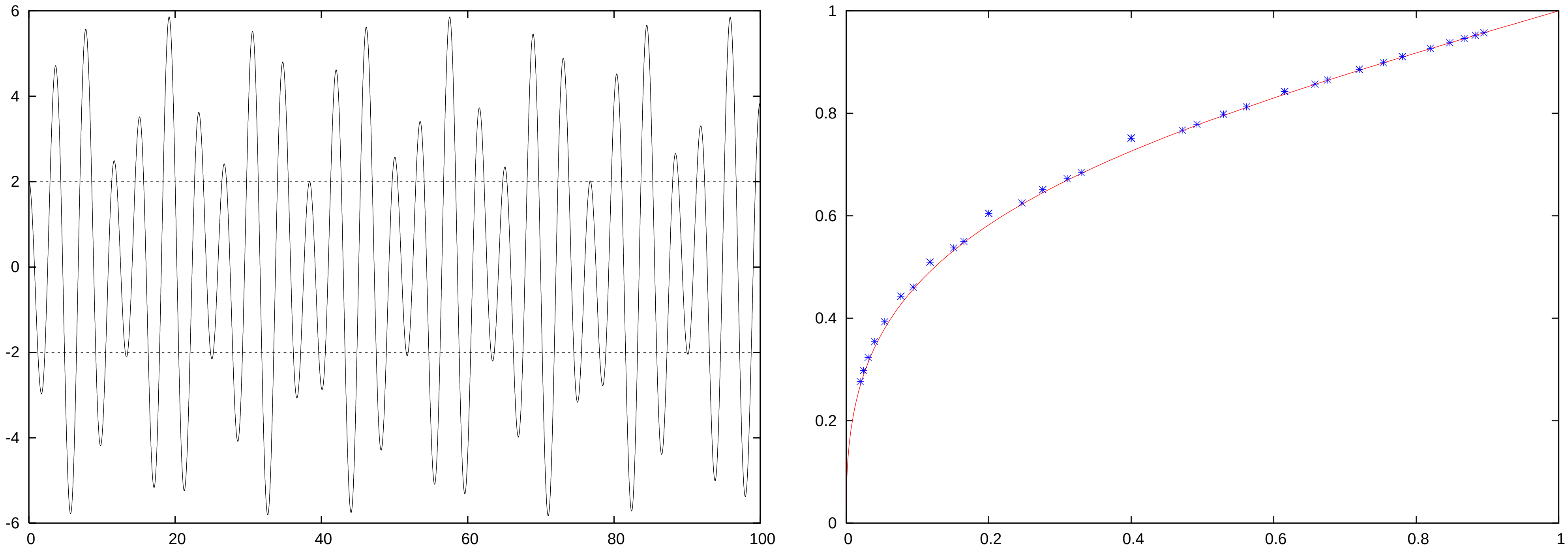

Left: behaviour of the **trace as a function of** $\sqrt{a}$ for $\delta = 0.06$. A **quasi-periodic pattern** is easily seen. Right: Plot of $\rho(\delta)$ for ω_2/ω_1 **irrational**. For completeness also the values for $\omega_2/\omega_1 = n/m$, $m \leq 10$, $0 < n < m$ are shown. Then δ has to **take the value** $2n^2/(m^2 + n^2)$.

The plot seems to show that the value of $\rho(\delta)$ in the rational case is **always larger than the values for nearby irrational cases**. This is illustrated in the next plot.

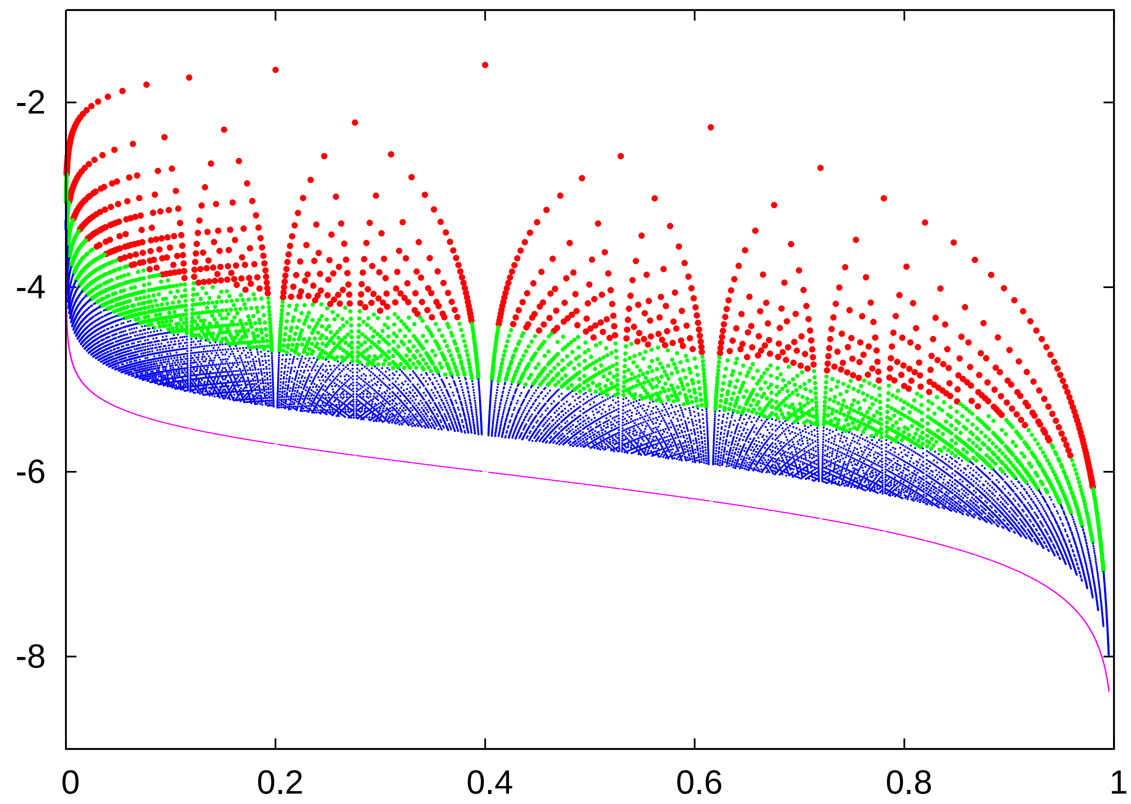

$\log_{10}(\rho_{\mathrm{rational}}(\delta) - \rho(\delta))$ **as a function of** δ **for the values of** δ **for which** $\omega_2/\omega_1 = n/m \in \mathbb{Q}$, $2 \leq m \leq 200$. The values of $m \leq 50$ (resp. $50 < m \leq 100$; resp. $100 < m \leq 200$) are plotted using large red (resp. medium size green; resp. small size blue) dots. One can check that, around a give value of δ, the difference is of order $\mathcal{O}(m^{-2})$. This can be checked even better in the lower line which displays $\log_{10}(\rho_{\mathrm{rat.}}(\delta) - \rho(\delta)) + 2\log_{10}(m) - 5$.

What about the zigzagging stability domains?

We want to study **several domains of positivity**. It is possible to reduce the study to

$$F_\omega = R_k \circ H_k \circ \ldots \circ R_2 \circ H_2 \circ R_1 \circ H_1$$

with all the R_j being **pure rotations** and the H_j **hyperbolic matrices** with **orthogonal eigenvectors** thanks to

Lemma *Let* $A = \begin{pmatrix} d & e \\ f & g \end{pmatrix}$ *be a symplectic matrix and assume* $\Sigma = d^2 + e^2 + f^2 + g^2 > 2$. *Then there exists matrices* $\bar{R}$ *and* H *satisfying* $A = \bar{R} \circ H$ *and such that* $\bar{R} = \begin{pmatrix} c & s \\ -s & c \end{pmatrix}$ *is a pure rotation, where* $c = \cos(\varphi)$, $s = \sin(\varphi)$, *for some suitable phase* φ, *and* H *is hyperbolic with orthogonal eigenvectors. Furthermore, among all possible decompositions of* A *as* $\bar{R} \circ H$, *the* H *with orthogonal eigenvectors is the one which maximises* $\operatorname{Tr} H$.

For each **hyperbolic matrix** H_j let E_j^s and E_j^u the **eigendirections** of H_j and S_j^s and S_j^u **symmetric sectors** around E_j^s and E_j^u of half width $1/\lambda_j$, where λ_j is the dominant eigenvalue.

Theorem 6 *Let $q = a + bp$ be $\mathcal{C}^2$ with $k \geq 1$ intervals of positivity. Let F_ω as before. Then the channels of stability of Hill's equation in the (a, b)-plane are close to curves for which $\arg R_j = \angle(E_j^u, E_{j+1}^s)$, where $E_m^{u,s}$ denote the unstable and stable directions of H_m. Furthermore the width of these channels is $O(\exp(-c(a^2 + b^2)^{1/4}))$ for suitable constants $c > 0$ and $a^2 + b^2$ large.*

It is clear that one should look for an **eigenvector with eigenvalue either $+1$ or -1**, to be at the **boundary** of an stability domain.

The proof follows by an analysis of **how different sectors** are mapped by the **successive hyperbolic matrices and the rotations**, by looking at expanding and contracting properties and by an **exponentially small tuning of one of the rotations**. In the proof we consider the case that only one of the rotations satisfies the condition. For the general case we proceed in a modified way.

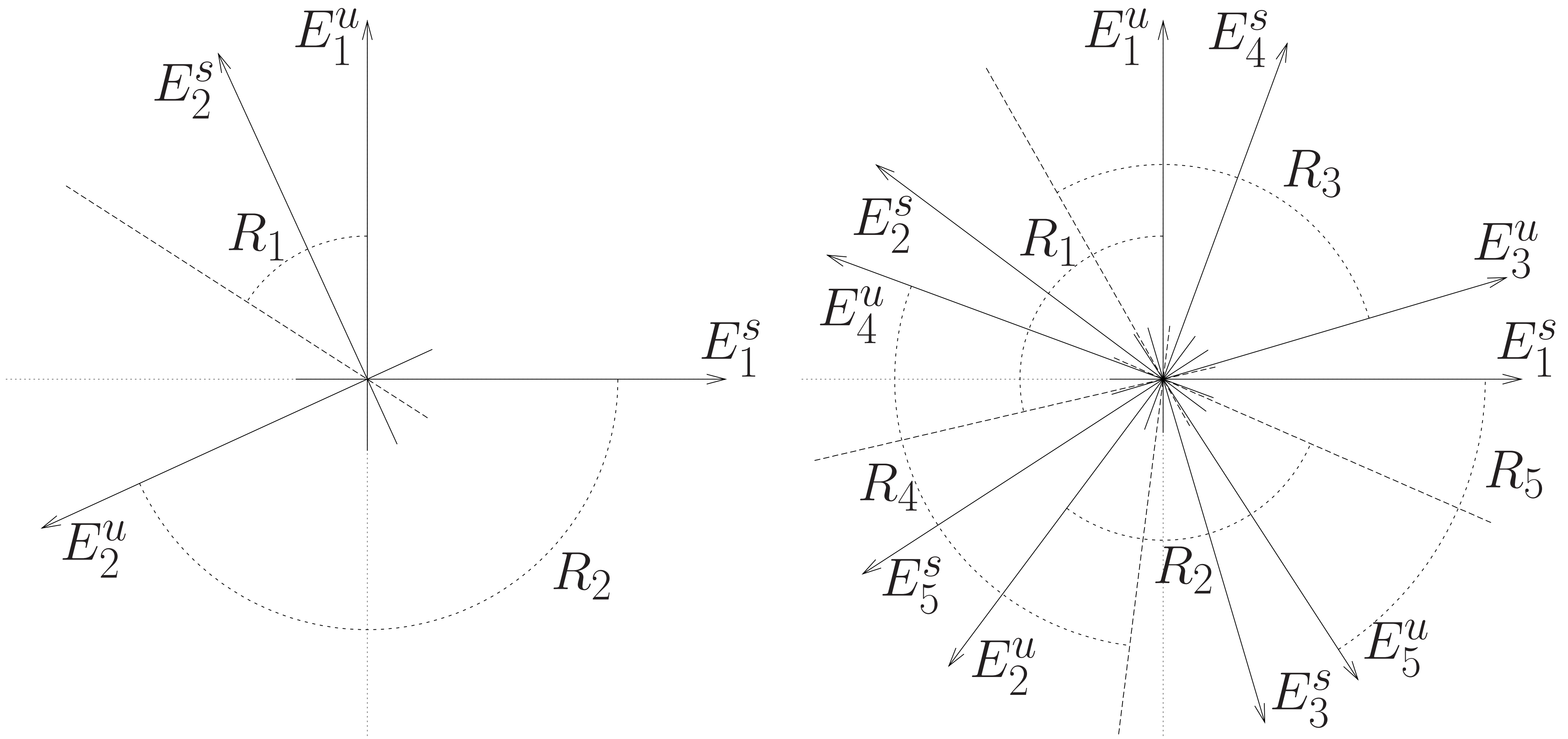

The **geometry of the different stable/unstable directions** of the H_j matrices and the **effect of the R_j rotations**. Left: $k = 2$. Right: $k = 5$. All the rotations are assumed to be counterclockwise.

We discuss on the **lattice-like behaviour of the stability domains**.

Theorem 7 *Assuming p of class C^2 with non-degenerate maxima and minima, the stability channels are centered about k $\mathbb{N}$-parametrised families of curves of the form*

$$\arg R_j(a,b) = \frac{\pi}{2}\frac{a+bp_M}{\sqrt{b|\ddot{p}(t_M)|}} = \alpha + \pi n + o((|a|+|b|)^0),$$

where $\alpha = \angle(E^u_j, E^s_{j+1})$, $n \in \mathbb{N} \cup \{0\}$. These curves are approximately parabolae, noting that the leftmost curve occurs for $n = 0$ and is very close to the line corresponding to a tangent maximum.

The proof is based on a computation of $\arg R_j(a,b)$.

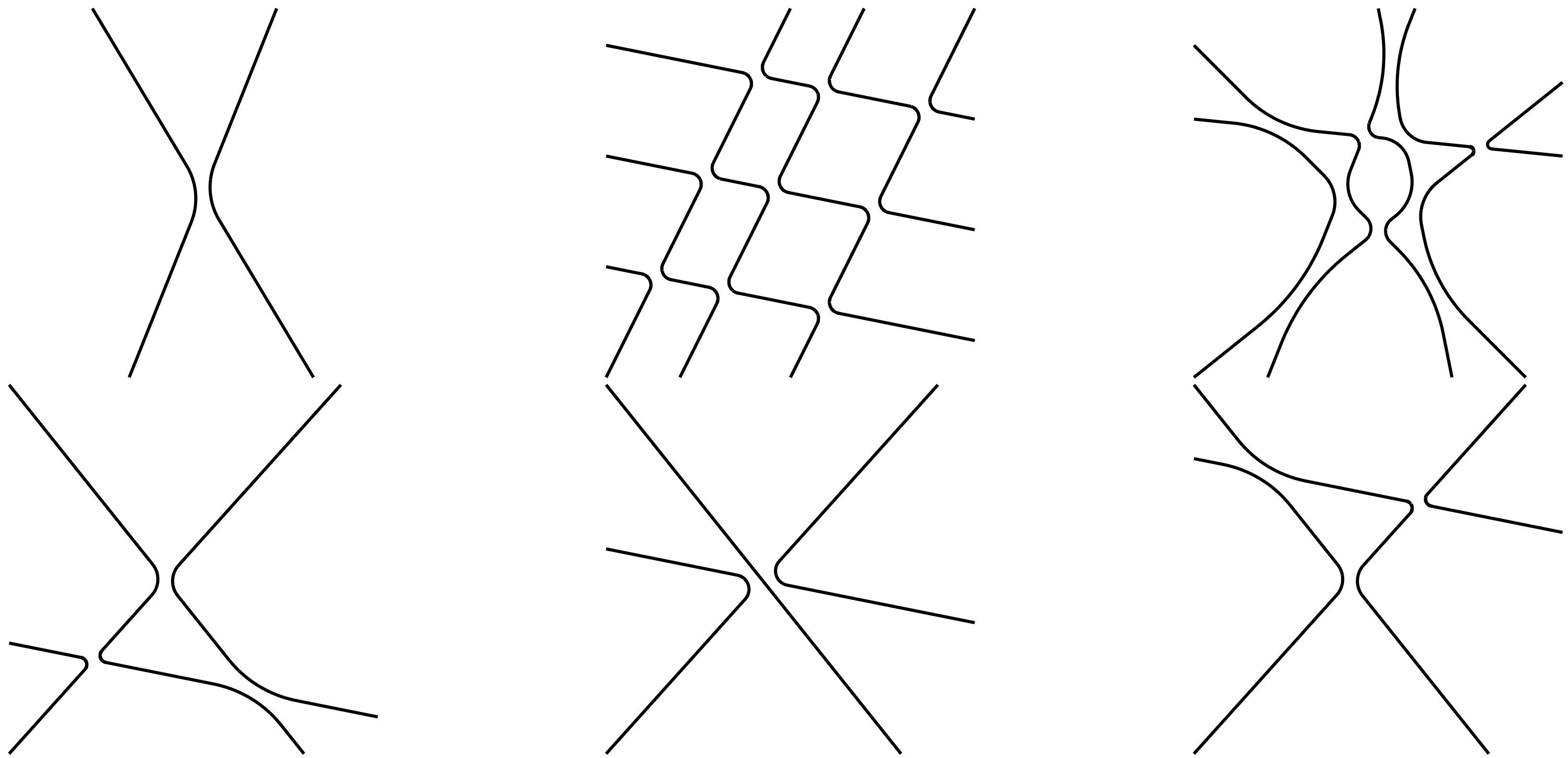

Top: An example of the **crossing of two lines** (left), **crossing of three lines of one family with three lines of another family** (middle) and **crossing of five lines** (right). The **zigzagging** behaviour is clearly seen in the middle plot. Bottom: sequences of the **evolution** during the **passage of a line** through the **crossing point of two other lines**. The analysis is done by using **rotation number**.

And beyond...

We can put the question: **what about the quasi-periodic case?**

That is, we replace the **periodic function** p by a **quasi-periodic one**.

This appears in a natural way to study the **stability properties of invariant tori** in some simple cases.

The problem appears in the form of **Hill-like equation**

$$\ddot{x} + (a + bp(t))x = 0,$$

or, in an equivalent way, as **1D Schrödinger equation**

$$-d^2u/d^2x + bp(x) = au.$$

In the **periodic** case we have **reducibility**.

In the **quasi-periodic** one, in general, **we do not have reducibility**.

We can consider the **discrete Schrödinger operators**

$$\left(H_{bV,\phi}x\right)_n = x_{n+1} + x_{n-1} + bV(\omega n + \phi)x_n = a x_n, \quad n \in \mathbb{Z}\,,$$

$V : (\mathbb{T})^d = (\mathbb{R}/2\pi\mathbb{Z})^d \to \mathbb{R}$ is a **potential**, $d \geq 1$, $b \in \mathbb{R}$ is a **coupling** parameter, $\phi \in \mathbb{T}^d$ is a **phase**, $\omega = (\omega_1, \ldots, \omega_d) \in \mathbb{R}^d$ is an **irrational frequency vector** and a is **the energy**.

As a first order system

$$\begin{pmatrix} x_{n+1} \\ x_n \end{pmatrix} = \begin{pmatrix} a - bV(\theta_n) & -1 \\ 1 & 0 \end{pmatrix} \begin{pmatrix} x_n \\ x_{n-1} \end{pmatrix}, \qquad \theta_{n+1} = \theta_n + \omega,$$

a **quasi-periodic skew-product** $\mathscr{M}$.

We shall just show

- A small **sample of potentials**,
- Some numerical illustrations of the **behaviour of the system**,
- An application to **nonlinear dynamics**.

We also shall comment on **the role of the number of frequencies**.

A sample of potentials

We shall consider simple potentials like

- The **Almost Mathieu, 1f**: $V(\theta) = \cos(\theta)$, $\theta = n\gamma$, $\gamma = (\sqrt{5}-1)/2$ understood theoretically. Used as a check of the algorithm.

- A **non-Morse potential, 1fm**:

$$V(\theta) = \cos\theta + \frac{1}{m}\left(\cos 2\theta + \cos 3\theta + \cos 4\theta\right),$$

  θ as before. For $m > 11$ this potential has only one maximum and one minimum, both non-degenerate. We choose $m = 2$.

- A **two-frequencies potential, 2f**:

$$V(\theta_1, \theta_2) = \cos\theta_1 + \cos\theta_2, \quad \theta_i = n\gamma_i, \quad \gamma = \left((\sqrt{5}-1)/2, \sqrt{3}-1\right).$$

- A **three-frequencies potential, 3f**:

$$V(\theta_1, \theta_2, \theta_3) = \cos\theta_1 + \cos\theta_2 + \cos\theta_3, \; \theta_i = n\gamma_i, \; \gamma = \left(\sqrt{2}-1, \sqrt{3}-1, \sqrt{5}-2\right).$$

We display: **resonances** (black), **KAM** (white between resonances), **"outer" uniformly hyperbolic** (white outside resonances), **non-reducible** (green).

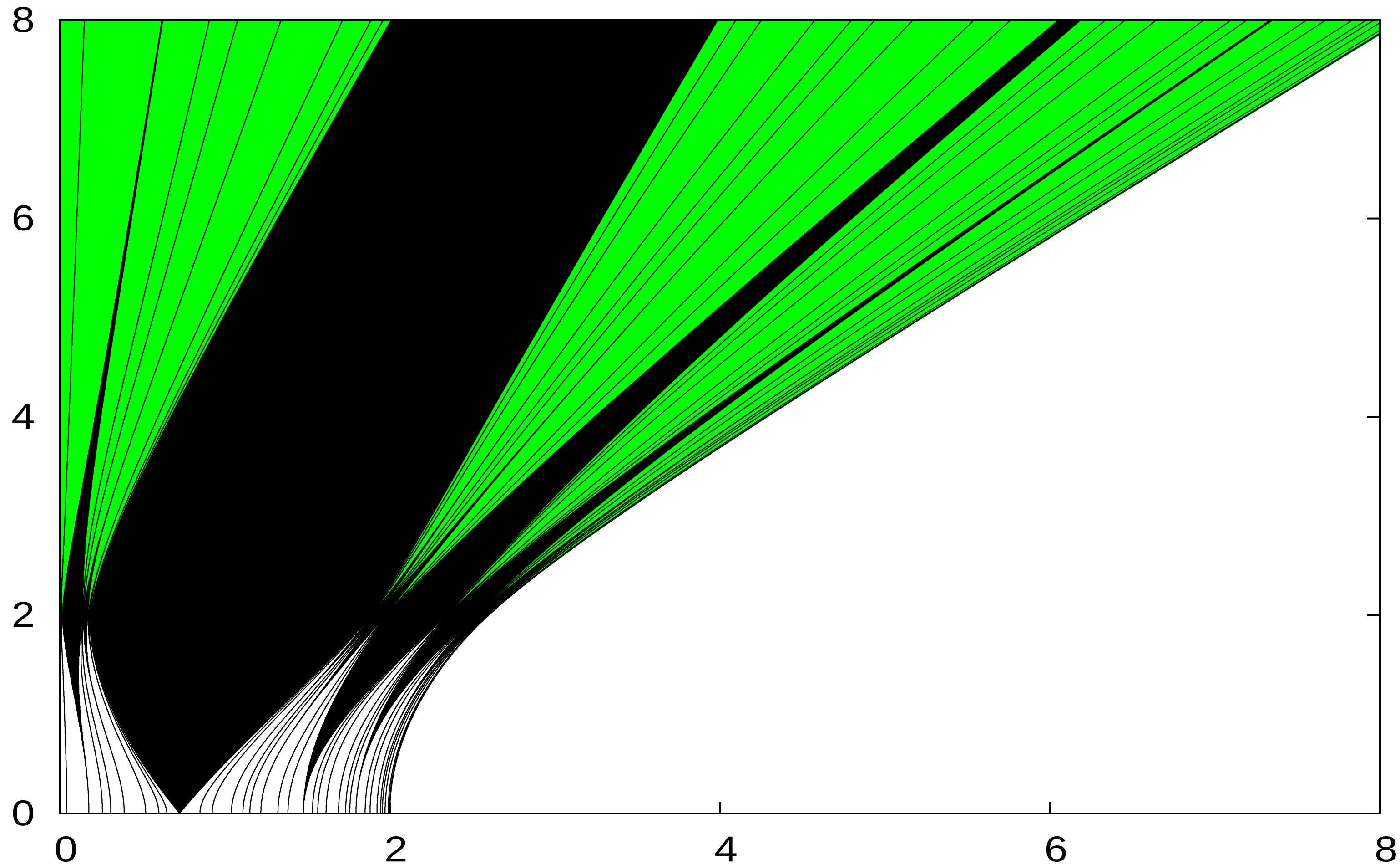

The **Almost Mathieu** model does not show **any collapsed gap**, the spectrum has **zero measure for $b = 2$**, it is **Cantor**. As a test, in **agreement with theoretical results**.

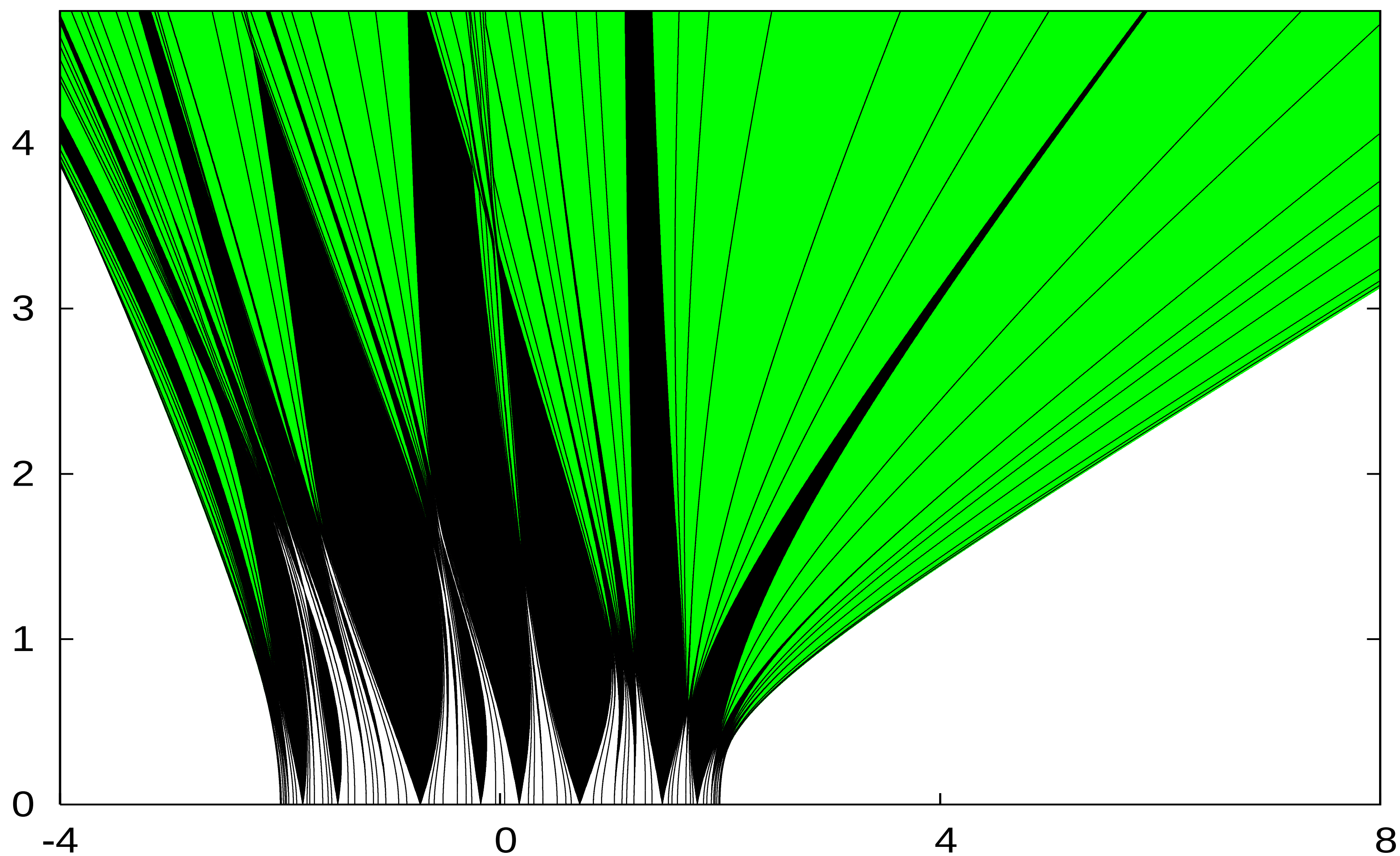

The **1fm** model **shows several collapsed gaps** of two types. When λ**=0** gaps collapse for a single b: **instability pockets**. (λ=Lyapunov exponent). When λ **>0** some resonance tongues **may collapse for a** b **interval** and then may **reopen** for a larger b. In all cases the collapse is **sharp**. There are sufficiently many open gaps to infer that the spectrum is **Cantor**.

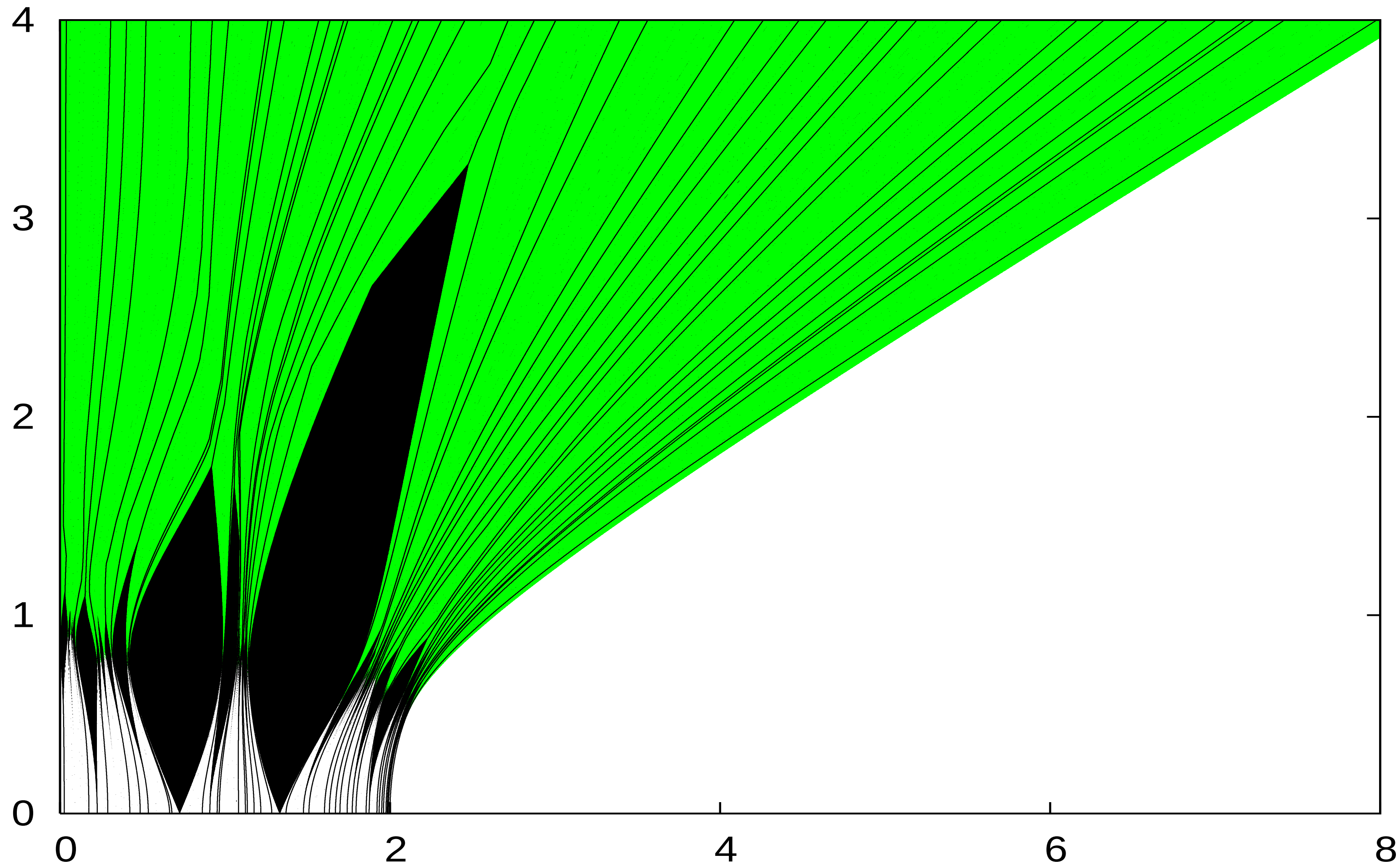

For the **2f** model and b **large enough** all gaps are **collapsed** and the spectrum consists of a single spectral band with $\lambda > 0$. The collapse is sharp. The **non-smooth character** also shows up at some places when the tongue is **still open** and $\lambda > 0$, the tongue boundaries being also non-smooth. For $\lambda = 0$ tongue boundaries are smooth and **pockets may appear**.

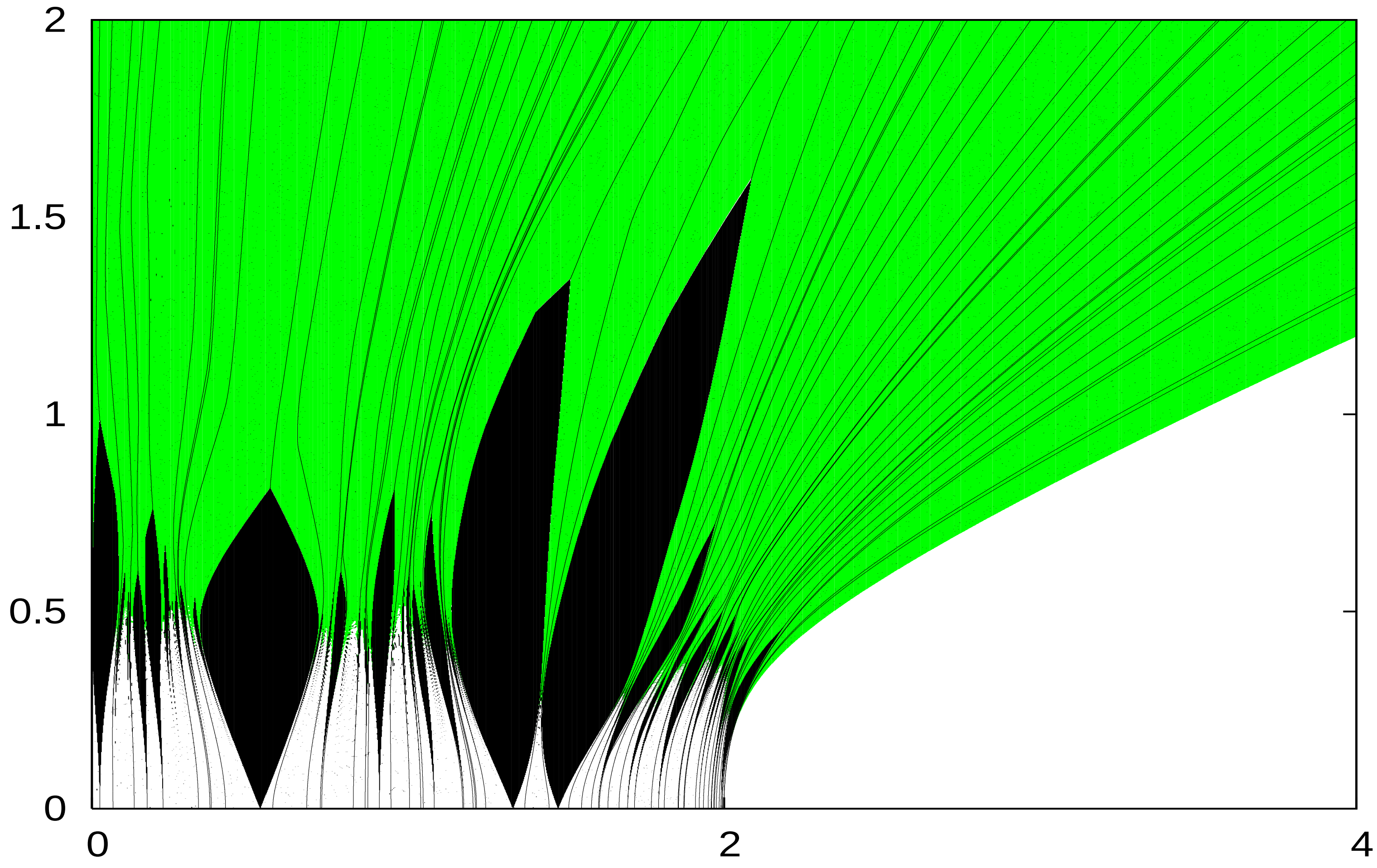

For the **3f** model the results are similar to the **2f** one. Compare with the **1f** ones.

In all cases we have proved that for **small b the boundaries are analytical**, having $\lambda = 0$. The cases **all Cantor gaps open** are characterised.

In all cases the simulations **agree** with the (scarce) **theoretical results**.

An application to nonlinear dynamics

The quasi-periodically driven Hénon dissipative map

Consider

$$H_{a,b,\gamma}\begin{pmatrix} x \\ y \\ \theta \end{pmatrix} = \begin{pmatrix} 1-(a+\varepsilon\cos(\theta))x^2+y \\ bx \\ \theta+2\pi\gamma \pmod{2\pi} \end{pmatrix},$$

that for $\varepsilon = 0$ is the well-known Hénon dissipative map. For $\varepsilon > 0$ it is known as the **q-p driven Hénon map**. Here γ=golden mean.

A first problem: Which is the **effect of q-periodicity** on the **period doubling cascade**? Is it possible to detect some **lack of reducibility**?

We fix the parameter b**=0.4** and look for **different values of** $\varepsilon > 0$ for increasing values of a.

Then, **for** $\varepsilon > 0$ **small** we have $\mathbf{2}^k$ **invariant curves**. The **linearized dynamics** is described by a **q-p skew product**.

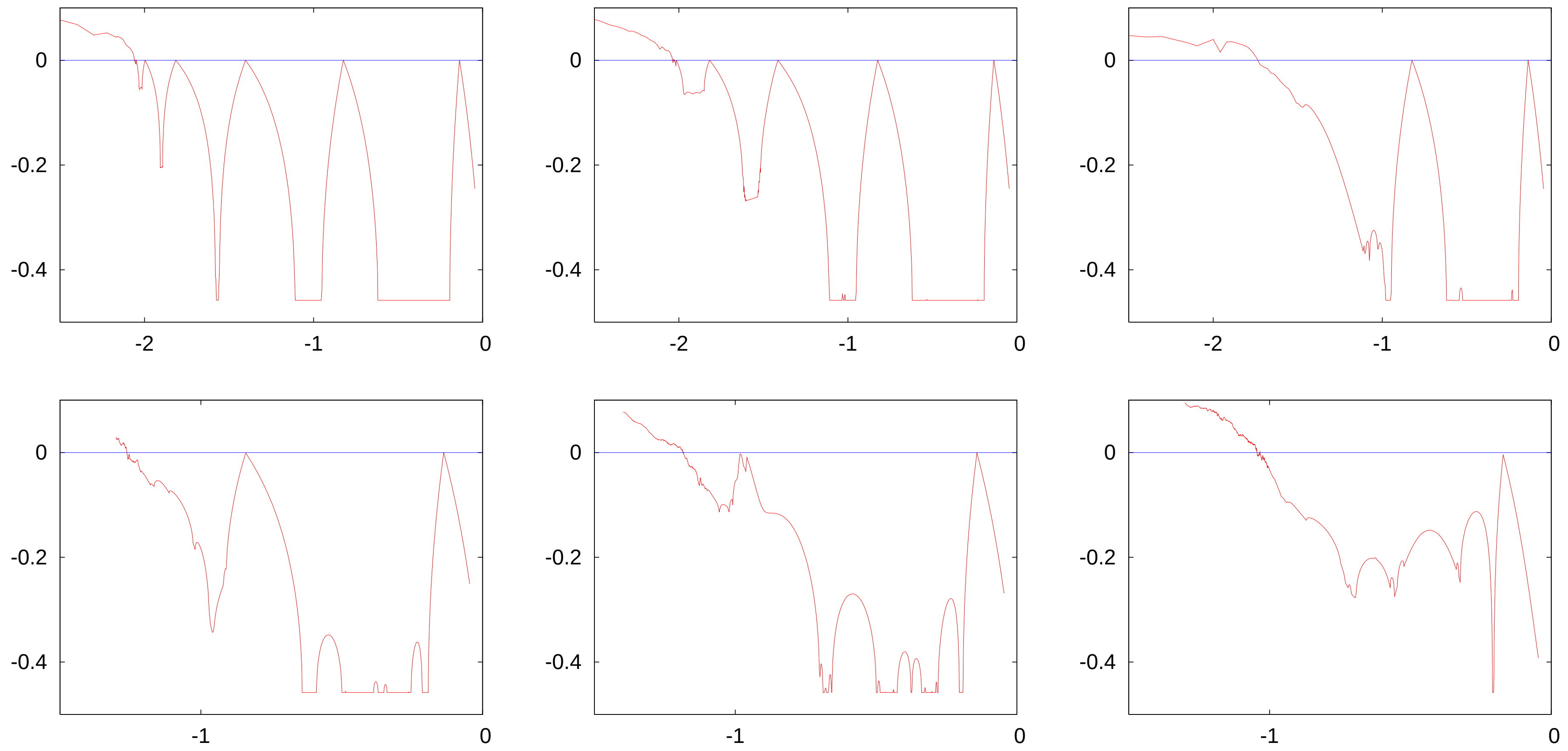

Variables plotted: λ **vs** $\log_{10}(1-a)$. ε**=0.0001,0.001,0.01** (top), ε**=0.05, 0.10,0.25** (bottom). Only a **finite number of period doublings** is seen.

Same phenomenon seen in many other cases from **3D diffeos to PDE**.

Bifurcations in the presence of **non-reducibility** should be one of the

New Trends in Dynamical Systems

Talk partially based on works with

H. Broer, M. Levi, J. Puig and R. Vitolo

Thanks for your attention!